ISSN 1027-5495. Functional Materials, 29, No.3 (2022), p. 346-358.
doi:https://doi.org/10.15407/fm29.02.346

Influence of pressure on the critical temperature and resistivity of $Y_{0.77}Pr_{0.23}Ba_2Cu_3O_{7-\delta}$ single crystals

***G.Ya.Khadzhai*[1], *Junyi Du*[1,2], *Z.F.Nazyrov*[1], *A.L.Solovyov*[1], *N.R.Vovk*[1], *R.V.Vovk*[1,3]**

[1]V.N.Karazin Kharkiv National University, 4 Svobody Sq., 61022 Kharkiv, Ukraine
[2]School of Mathematical Sciences, Luoyang Normal University, 471934 Luoyang, China
[3]Ukrainian State University of Railway Transport, 7 Feyerbaha Sq., 61050 Kharkiv, Ukraine

Received January 12, 2022

n the present work, we investigated the influence of high hydrostatic pressure up to 11 kbar on the conductivity in the basal *ab*-plane of $Y_{1-x}Pr_xBa_2Cu_3O_{7-\delta}$ single-crystalline samples medium-doped with praseodymium ($x \approx 0.23$). It was found that, in contrast to the pure $YBa_2Cu_3O_{7-\delta}$ with the optimal oxygen content, the application of high pressure leads to phase separation in the basal plane of $Y_{0.77}Pr_{0.23}Ba_2Cu_3O_{7-\delta}$ single crystals. Possible mechanisms of the effect of praseodymium doping and high pressure on the two-step transition to the superconducting state are discussed. It was established that in the normal state, there is a conductivity of the metallic type, limited by the scattering of phonons (Bloch-Gruneisen regime) and defects. The fluctuation conductivity is considered within the Lorentz-Doniach model. Hydrostatic pressure, accompanied by a decrease in anisotropy, leads to a decrease in the residual and phonon resistances. The Debye temperature and coherence length are independent of pressure. The applicability of the McMillan formula in the presence of significant anisotropy is discussed. The excess conductivity $\Delta\sigma(T)$ obeys an exponential temperature dependence in the broad temperature range $T_f < T < T^*$. The dependence $\Delta\sigma(T) \sim (1 - T/T^*)\exp(\Delta^*_{ab}/T)$ is interpreted in terms of the mean-field theory, where T^* is the mean-field temperature of transition to the pseudogap state; and the temperature dependence of the pseudogap is satisfactory described within the BCS-BEC crossover theory.

Keywords: YPrBaCuO single crystals, doping, hydrostatic pressure, anisotropy, excess conductivity, scattering, Debye temperature.

Вплив високого тиску на електропровідність в базовій площині монокристалів $Y_{0.77}Pr_{0.23}Ba_2Cu_3O_{7-\delta}$. *Г.Я.Хаджай, С.Н.Камчатна, М.Коробков, Я.Нечепоренко, М.Р.Вовк, Р.В.Вовк,*

В роботі досліджено вплив високого гідростатичного тиску до 12 кбар на електроопір у базовій *ab*-площині середньолегованих празеодимом ($x \approx 0.23$) монокристалів $Y_{1-x}Pr_xBa_2Cu_3O_{7-\delta}$. Виявлено, що, порівняно зі зразками чистого $YBa_2Cu_3O_{7-\delta}$ з оптимальним вмістом кисню, застосування високого тиску призводить до потрійного зростання величини баричної похідної dT_c/dP і зміщення температури точки 2D–3D кросовера. Обговорюються можливі механізми впливу високого тиску на T_c, з урахуванням наявності особливостей в електронному спектрі носіїв заряду, який характерний для решіток із сильним зв'язком. Встановлено, що надлишкова електропровідність $\Delta\sigma(T)$ монокристалів $Y_{0.77}Pr_{0.23}Ba_2Cu_3O_{7-\delta}$ має експоненціальну температурну залежність у

широкому діапазоні температур $T_f < T < T^*$. Надлишкова провідність може бути описана співвідношенням $\Delta\sigma(T) \sim (1 - T/T^*)\exp(\Delta^*_{ab}/T)$ та інтерпретована у термінах теорії середнього поля, де T^* — середньопольова температура переходу в псевдощілинний стан; температурна залежність псевдощілини задовільно описується у межах теорії кросовера БКШ-БЄК. Збільшення тиску, що додається, призводить до ефекту звуження температурного інтервалу реалізації псевдощілини.

1. Introduction

The use of high-pressure technologies to study the critical characteristics of HTSC materials continues to be one of the most promising experimental techniques that allow not only testing the adequacy of numerous theoretical models but also finding empirical ways to improve their electrical transport characteristics and increase critical parameters [1, 2]. The latter circumstance seems to be especially important, given the fact that, despite a 35-year history of intensive theoretical and experimental research, starting from the discovery of HTSC in 1986 [3], it has not been possible to overcome the critical temperature threshold of 200 K, not to mention room temperature superconductivity for superconducting materials [4, 5]. At the same time, the microscopic mechanism of HTSC still remains unclear [1, 6].

In a fairly numerous series of HTSC cuprates, the special place for research, in this aspect, is occupied by the compound of the 1-2-3 system with partial replacement of yttrium by praseodymium [7, 8], which is due to several reasons. First, the compounds of the 1-2-3 system have a sufficiently high critical temperature (T_c), which makes it possible to carry out measurements at temperatures exceeding the temperature of liquid nitrogen [9, 10]. Second, the partial replacement of yttrium with praseodymium, in contrast to replacement with other rare earth elements, makes it possible to smoothly change the electrical resistance and critical characteristics of this compound due to the gradual suppression of their conductive parameters (the so-called "praseodymium anomaly") [11–14]. Thirdly, in the $Y_{1-x}Pr_xBa_2Cu_3O_{7-\delta}$ compounds with an optimal oxygen content [15, 16], the so-called nonequilibrium state does not arise, which in pure oxygen-deficient $YBa_2Cu_3O_{7-\delta}$ samples can be quite easily induced by a jump in temperature, aging [17, 18] or high-pressure applications [19, 20]. The latter circumstance is essential, since, in the case of pure samples, it is often necessary to use specific techniques that allow one to isolate the so-called "true pressure effect" due to a change in the crystal lattice parameters of the interlayer interaction, electron-phonon interaction, etc. [21, 22], and relaxation effect due to the redistribution of the labile component [23, 24]. Despite a relatively large number of works available in the literature on the study of the effect of pressure on the conductivity of the HTSC cuprates, only a relatively small part of them was devoted to the study of the pressure dependences of the resistive characteristics and the shape of superconducting transitions of $Y_{1-x}Pr_xBa_2Cu_3O_{7-\delta}$ compounds (see, for example, review [7] and links there). Moreover, the data presented in these works are often quite contradictory. For example, it was reported that both the positive and negative baric derivative dT_c/dP were recorded, and in some cases, the sign of dT_c/dP changed [25].

At the same time, the approximation of the temperature dependence of the resistivity using the known mechanisms of charge carrier scattering in the normal state and during the transition to the superconducting state makes it possible to obtain a number of characteristic parameters, to relate them to each other, and also to study the influence of external factors on the scattering processes and the transition to the superconducting state. In the normal state, these are known mechanisms of carrier scattering by phonons and lattice defects.

In our previous works [26, 27], we studied the effect of high hydrostatic pressure up to 17 kbar on a number of resistive characteristics and excess conductivity of single crystal $Y_{1-x}Pr_xBa_2Cu_3O_{7-\delta}$ samples poorly doped with praseodymium ($x \approx 0.05$). In this work, we investigated the effect of high hydrostatic pressure up to 11 kbar on the phase separation in the basal *ab*-plane of $Y_{1-x}Pr_xBa_2Cu_3O_{7-\delta}$ single-crystal samples moderately doped with praseodymium ($x \approx 0.23$). We approximate the resistivity temperature dependence in the range T_c — 160 K using the Bloch-Gruneisen relation with the transition to fluctuation conductivity described in accordance with the Lorentz-Doniach results.

HTSC $Y_{1-x}Pr_xBa_2Cu_3O_{7-\delta}$ single crystals were grown by the solution-melt technology in a gold crucible, according to the proce-

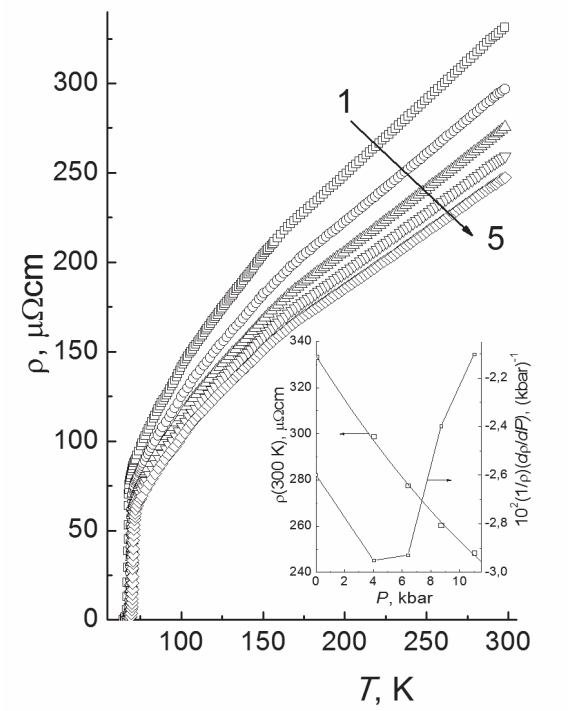

Fig. 1. Electrical resistance of the $Y_{0.77}Pr_{0.23}Ba_2Cu_3O_{7-\delta}$ single crystal in the basal plane, $\rho_{ab}(T, P)$, for: *1* — $P = 0$; *2* — $P = 4$; *3* — $P = 6.4$; *4* — $P = 8.7$; *5* — $P = 11$ kbar. Insert: Temperature dependences $\rho_{ab}(300, P)$ and derivative, $(d[\ln\rho_{ab}(300, P)])/dP$.

dure [26]. For resistive studies, rectangular crystals with a size of 3×0.5×0.03 mm³ were selected. The smallest crystal size corresponds to the *c*-axis direction. According to the standard 4-contact scheme, electrical contacts made of silver paste were deposited on the crystal surface; then, silver conductors with a diameter of 0.05 mm were attached and annealed for three hours at a temperature of 200°C in an oxygen atmosphere. This procedure made it possible to obtain a contact resistance of less than one Ohm and to carry out resistive measurements at transport currents up to 10 mA in the *ab*-plane. Hydrostatic pressure was created in a piston-cylinder multiplier [26, 27]. The pressure was determined using a manganin manometer, and the temperature was measured with a copper-constantan thermocouple mounted on the outer surface of the chamber at the level of the sample position.

The temperature dependences of the electrical resistivity $\rho_{ab}(T,P)$ in the basal plane of the $Y_{0.77}Pr_{0.23}Ba_2Cu_3O_{7-\delta}$ single crystal measured at different pressures (from $P = 0$ to 11 kbar, see also table) are shown in the

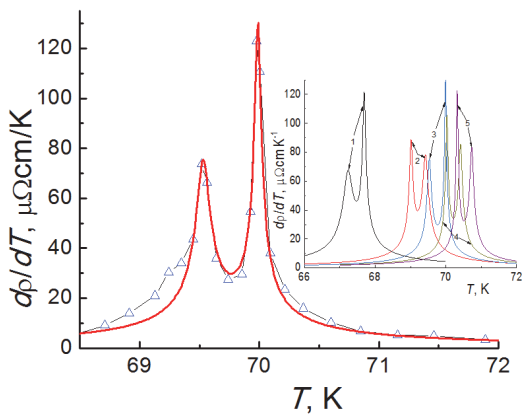

Fig. 2. Derivative, $d\rho_{ab}(T, 6.4\ \text{kbar})/dT$, in the superconducting transition region: points — calculated from experimental data $\rho_{ab}(T, 6.4\ \text{kbar})$. Line: empirical distribution function (*1*). Box: empirical distribution functions (*1*) for the pressures used (see caption to Fig. 1).

inset to Fig. 1. At atmospheric pressure, $T_c(0) \approx 67$ K and ρ_{ab} (300 K, 0) ≈333 μOhm·cm were measured. Thus, in comparison with the pure $YBa_2Cu_3O_{7-\delta}$ single-crystal samples, the critical temperature decreased by ≈ 25 K with a simultaneous increase in ρ_{ab} (300 K, 0) by ≈120 μOhm·cm, which generally agrees with the literature data. The reasons for the deterioration of the conducting characteristics of $YBa_2Cu_3O_{7-\delta}$ compounds upon doping with praseodymium ("praseodymium anomaly") are analyzed in detail in the review [7].

The inset to the figure 1 shows the pressure dependence of the resistance at room temperature, $\rho_{ab}(300, P)$, and the derivative, $d[\ln\rho_{ab}(300, P)]/dP$. The ρ_{ab} depends on pressure primarily due to a decrease in volume, that is, due to an increase in the Debye temperature, θ, and, at sufficiently high temperatures, $\rho \propto \theta^{-2}$.

Then $d(\ln\rho_{ab})/d(\ln V) = [d(\ln_{ab})/d(\ln\theta)]/[d(\ln\theta)/d(\ln V)] \approx -2\gamma$ [28] and $(1/\rho)(d\rho/dP) = 2\gamma\beta$, where $\beta = -(1/V)(dV/dP)$.

It is seen that the value $(1/\rho)(d\rho/dP) = 2\gamma\beta$ varies within 3÷2 (kbar)$^{-1}$, which for $\gamma \approx 2$ gives the value of the volumetric compressibility, $\beta \approx 0.005 \div 0.007$ (kbar)$^{-1}$. These values are in qualitative agreement with the data of [29], in which the value $\beta \approx 0.0085$ was obtained for $YBa_2Cu_3O_x$. The decrease in the compressibility of our sample can be due to both by the presence of praseodym-

Table 1. Parameters of the empirical distribution function (1)

	P, kbar	0	4.1	6.4	8.7	11
Low	T_{cl}, K	67.23	69.0135	69.530	70.027	70.320
	w_l, K	24.37	8.61	10.98	6.15	5.13
	b_l, μΩ·cm·K	949	454	524	415	408
	$(d\rho/dT)_{lmax}$	67.5	88.8	75.6	105.73	122.57
High	T_{ch}, K	67.69	69.422	69.988	70.413	70.729
	w_h, K	8.28	14.87	5.20	9.85	10.15
	b_h, μΩ·cm·K	601	726	447	542	550
	$(d\rho/dT)_{hmax}$	121.91	78.3	130.3	85.8	83.6

ium and by the inhomogeneity of the sample itself (see Fig. 2).

High-temperature superconductors are characterized by the presence of microscopic regions (domains) [30] with different T_c. Thus, there is a distribution of T_c over the sample volume. This inhomogeneity of the sample leads to an extension of the range of the superconducting transition to 0.1÷1 K in optimally doped HTSCs [31]. Note that the measured effective resistance decreases with decreasing temperature, since a single superconducting cluster consisting of domains that have already passed into the superconducting state grows; and in the absence of percolation effects, the decrease in the resistance near the superconducting transition is proportional to the total volume fraction of domains that have already become superconducting at a given temperature, $T \le T_{ci}$. Under these conditions,the only experimentally determined characteristic temperature in the region of the superconducting transition is the temperature of the maximum of the derivative, $d\rho/dT$, and the derivative itself, $d\rho(T \approx T_c)/dT$, is proportional to the distribution function for T_{ci} [32, 33]. Note that the effective resistance vanishes only when a single cluster formed from superconducting domains extends from one potential contact to another. Since the distribution function for T_{ci} is related to the heterogeneity of a particular sample, it is a characteristic of the sample, and therefore, it should be determined by approximating the function $F(T) = d\rho\ (T \approx T_c)/dT$ using good empirical relationships.

In lightly doped samples and samples with defects (impurities, substitutional atoms, etc.), macroscopic regions with their own distributions of T_c over the volume of the region can form, which leads to a multistage superconducting transition [34]. In this case, according to the well-known parabolic dependence [35], each of these phases is characterized by the corresponding concentration of current carriers. In this case, the distribution function for T_{ci} is the sum of the corresponding functions $F_i(T)$.

Fig. 2 shows the derivative $d\rho_{ab}(T)/dT$ in the superconducting transition region for one of the pressures (6.4 kbar) and the corresponding empirical distribution function. For the latter, we used the sum $F(T) = F_i(T) + F_h(T)$, where $F_i(T)$ and $F_h(T)$ have the next form

$$F_i(T) = \frac{b_i}{\sqrt{(T^2 - T_{ci}^2)^2 + (w_i T)^2)}}. \quad (1)$$

Here $i = h,\ l$; T_{ci}, b_i and w_i are parameters determined by the least-squares method. The average approximation error is close to 3 %. The values of these parameters are presented in Table 1.

Fig. 2 shows that the empirical distribution function (1) describes well the derivative, $d\rho_{ab}(T,\ 6.4\ \text{kbar})/dT$, in the entire region of the superconducting transition, except for the lowest-temperature region $T < 69.5$ K, where there is another distribution of type (1), whose parameters are difficult to determine due to the small number of experimental points.

Insert in Fig. 2 demonstrates the shift of the maxima $d\rho_{ab}(T,\ P)/dT$ towards higher temperatures in the region of the superconducting transition upon application of hydrostatic pressure. In this case, the heights of the maxima change arbitrarily, i.e. with each stage of cooling, its own distribution of T_c is created, which only qualitatively corresponds to the previous one. It can be seen from the Table 1 that only T_{ci} increases with increasing pressure. The parameters b_i and w_i are independent of pres-

sure. An exception is a height of the lower-temperature maximum, $(d\rho/dT)_{lmax}$, which tends to increase with increasing pressure. Such a change in the steepness of the steps indicates a change in the paths of current flow after annealing the crystals at room temperature, which is possible with a change in the spatial distribution of clusters and their sizes for the low-temperature and high-temperature phases.

The width of the superconducting transition is determined by the inhomogeneity of the sample — for example, fluctuations of its composition [36]. These inhomogeneities lead to the appearance of regions with their own local transition temperature, and the transition in these regions occurs regardless of the state of neighboring regions. As noted above, the homogeneous state of HTSC with defects is unstable; it is energetically favorable to split HTSC into domains $l \sim 10^{-5}$ cm in size with high and low conductivities (metallic regions with small δ and poorly conducting regions with large δ). For the case of ferroelectric phase transitions, such regions are called Kenzig regions [37], the size of which is also estimated as $l \sim 10^{-5} \div 10^{-6}$ cm, ($a << l << L$; where a is the crystal lattice constant, L is the sample size). It can be assumed that the width of the step of the one-step superconducting transition — the width of one maximum $d\rho_c(T)/dT$ at half its height — is determined precisely by such mesoscopic fluctuations in the concentration of defects oxygen vacancies or impurity atoms.

The appearance of a two-step superconducting transition (two maxima $d\rho_c(T)/dT$)) after doping with praseodymium indicates the appearance of at least two macroscopic regions with different, lower than in the initial state, transition temperatures. It is clear that each of these regions has its own transition width generated by mesoscopic fluctuations in the concentration of defects in this region.

Note that the disappearance of resistance is due to the formation of a single superconducting cluster extending from one potential contact to another and shunting all the others, both normal and superconducting regions. Thus, doping with praseodymium led to the appearance, along with mesoscopic, macroscopic inhomogeneities, which caused a two-step superconducting transition, shifted to the region of lower temperatures, and the steps of which expand with an increase in the concentration of praseodymium. Thus, the spatial distribution of defects created by the praseodymium impurity leads to the fact that, along with mesoscopic fluctuations, macroscopic fluctuations in the concentration of defects are also observed. It is most likely that such macroscopic regions with different defect concentrations are separate phase clusters in the *ab*-planes of the $YBa_2Cu_3O_{7-\delta}$ single crystal.

A similar temperature dependence of the resistance was found in [38] for an amorphous Zr–Rh alloy in the range 4.8–298 K and is attributed to a possible spatial inhomogeneity of this alloy. In [30], referring to the experimental data on the separation of $La_2CuO_{4+\delta}$ into large metallic regions and small dielectric regions (the size of the regions is ~ 10^{-5} cm), the authors substantiate the energetic advantage of separating HTSC into domains with high and low conductivities. Naturally, the separation process is controlled by the diffusion of the corresponding ions, which is relatively low even near room temperatures. Nevertheless, the homogeneous state of HTSC with defects is unstable according to [30].

The phase separation under pressure observed in our case can be associated with different sizes and compositions of clusters with different praseodymium content [7]. At the same time, it should be noted that an increase in the praseodymium content in a local volume element, as a rule, leads to a diametrically opposite effect of an increase in the oxygen content. While an increase in the oxygen concentration leads to an increase in T_c and an improvement in the conducting characteristics of an individual phase [17], an increase in the praseodymium content contributes to the suppression of conductivity and a decrease in T_c [7]. The structural and kinematic anisotropy in the system can play a special role in this [39–43]. It can be assumed that in contrast to the case of pure $YBa_2Cu_3O_{7-\delta}$ samples, the phase separation observed in the $Y_{0.77}Pr_{0.23}Ba_2Cu_3O_{7-\delta}$ single crystal under high pressure is a more complex and ambiguous process. However, to verify the validity of this assumption, additional studies are needed on the effect of all-round compression on the critical temperature of $Y_{1-x}Pr_xBa_2Cu_3O_{7-\delta}$ compounds, including a wider range of praseodymium concentrations, as well as using structural measurements on samples with a higher degree of doping with praseodymium.

The dependences of the transition temperatures on the applied pressure for

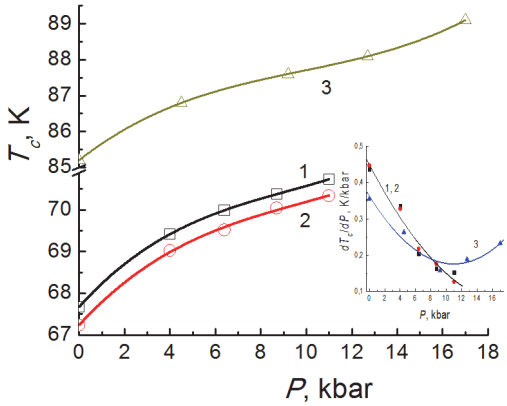

Fig. 3. Pressure dependences of the superconducting transition temperatures: *1* — T^{high}, *2* — T^{low}, *3* — $Y_{0.95}Pr_{0.05}Ba_2Cu_3O_{7-\delta}$ [20]. Inset: Pressure dependences of the derivatives dT_c/dP for $Y_{1-x}Pr_xBa_2Cu_3O_{7-\delta}$ single crystals ($x = 0.23$, $x = 0.05$). Numbering of the curves is the same as in the main panel).

$Y_{1-x}Pr_xBa_2Cu_3O_{7-\delta}$ single crystals ($x = 0.23$ in this work, $x = 0.05$ from [20]) are presented in Fig. 3. The pressure dependences of the corresponding derivatives $(dT_c/dP)(P)$ are shown in the inset to Fig. 3. The curves $T_c^{high}(P)$ and $T_c^{low}(P)$ are nearly parallel to each other. This means that an increase in the pressure does not result in a notable change of the difference $T_c^{high} - T_c^{low}$ (see Table 1), which may indicate the preservation of the initial phase segregation in the crystal. It should be noted that the oxygen content in our sample is close to the stoichiometric one, which should minimize the redistribution of the labile oxygen in the above-described processes. Indeed, as shown in [1, 2, 17, 19], in the case of stoichiometric single crystals, application of high pressure usually does not cause structural relaxation processes due to the diffusion of labile oxygen in the bulk of the sample.

Phase segregation in our sample under pressure is probably due to the different size and composition of clusters with different concentrations of Pr [7, 11]. At the same time, one should note that an increase in the Pr content in the local volume of the experimental sample leads, as a rule, leads to an effect opposite to the effect of an increase in the oxygen content. If an increase in the oxygen concentration leads to an increase of T_c and improvement of the conducting characteristics of a given phase [1, 16, 17], an increase of the Pr content contributes to a suppression of the conductivity and a decrease in T_c [7, 11, 14, 20]. In this way, one can assume that the phase segregation observed in the $Y_{0.77}Pr_{0.23}Ba_2Cu_3O_{7-\delta}$ single crystal under pressure is a more complex and ambiguous process in contrast to $YBa_2Cu_3O_{7-\delta}$ single crystals without Pr. Verification of this assumption requires additional studies of the effect of uniform compression on T_c of $Y_{0.77}Pr_{0.23}Ba_2Cu_3O_{7-\delta}$ compounds in a wide range of Pr concentrations in combination with the structural characteristics of samples with a higher level of Pr doping.

We note that T_c increases with increasing pressure. Specifically, the curves $T_c(P)$ for $x \approx 0.23$ pass below those for $x \approx 0.05$ [20]. Qualitatively, this observation agrees with the data [7] for $Y_{1-x}Pr_xBa_2Cu_3O_{7-\delta}$ composites. The inset to Fig. 3 shows that dT_c/dP decreases almost linearly with increasing pressure, but at the highest pressures an increase is observed. At the same time, for $Y_{0.95}Pr_{0.05}Ba_2Cu_3O_{7-\delta}$ [15, 20], the pressure dependences of dT_c/dP pass through a minimum at $P \approx 10$ kbar. Probably, such a minimum can be expected for $Y_{0.77}Pr_{0.23}Ba_2Cu_3O_{7-\delta}$ at even higher pressures.

The temperature dependence of the sample resistivity was approximated by the relations:

$$\rho_{ab}(T) = (\rho^{-1} + \Delta\sigma_{LD})^{-1}; \qquad (2)$$

$$\rho = (\rho_0 + \rho_3 + \rho_5) \cdot (1 - b_0 \cdot T^2);$$

$$\rho_n = C_n \left(\frac{T}{\theta}\right)^n \int_0^{\theta/T} \frac{x^n e^x}{(e^x - 1)^2} dx;$$

$$\Delta\sigma_{LD} = \left(\frac{e^2}{16hd}\right)\varepsilon^{-1}(1 + J\varepsilon^{-1})^{(-1/2)};$$

Here ρ_0 is the residual resistivity due to the scattering of charge carriers on defects; ρ_3, ρ_5 are the resistivities due to scattering of charge carriers by phonons (Bloch-Gruneisen (regime) relation): ρ characterizes the interband scattering and ρ_5 is the intraband scattering [44]; b_0 characterizes the change in the shape of the curve of the density of electronic states with increasing temperature [45]; $\Delta\sigma_{LD}$ is the Lawrence-Doniach excess conductivity [46]; d is the interplanar distance in the $Y_{0.77}Pr_{0.23}Ba_2Cu_3O_{7-\delta}$ single crystal; $\varepsilon \approx (T-T_c)/T_c$; $J = (2\xi_c(0)/d)^2$ is the interplanar pairing constant, ξ_c is the coherence length along the c axis. The temperature of the superconducting (SC) transi-

Table 2. Parameters of the approximation according to (2), relative decrease in volume and interplanar spacings calculated using [47] and $\xi_c(0)$ values for various applied pressures

P, kbar	0	4.1	6.4	8.7	11
T_c^{high}, K	67.67	69.42	69.98	70.38	70.73
T_c^{low}, K	67.23	69.02	69.52	70.04	70.33
θ, K	279	284	281	279	279
T_c^{high}/θ	0.242	0.244	0.249	0.252	0.254
ρ_0, μOhm·cm	58	49	35	34	37
C_3, μOhm·cm	71	60	68	65	31
C_5, μOhm·cm	1456	1462	1369	1244	1199
b_0, 10^{-6}, K^{-2}	3.1	4.2	5.4	4.8	4.0
J	14.4	7.2	21	18.5	11.4
$\xi_c(0)$, Å	22	15	26	24	19
Error, %	1.5	1	1.5	1.5	1.5

tion was determined experimentally from the position of the maximum $d\rho(T)/dT$. The parameters of the approximation according to (2) are given in Table 2, together with the values of the relative decrease in volume and interplanar spacing calculated from the data of [47], as well as the values of $\xi_c(0)$.

Fig. 4 shows the $\rho_{ab}(T)$ dependences at various pressures and the corresponding approximating curves for the $Y_{0.77}Pr_{0.23}Ba_2Cu_3O_{7-\delta}$ single crystal. It can be seen that the $\rho_{ab}(T)$ dependence does not qualitatively change at all applied pressures and remains metallic. At the same time, the parameters of the approximation according to (2) are changed (see Table 2). Inset *a* shows the SC transition at one of the pressures (11 kbar). The total width of the transition (~ 3 K) and the presence of steps on it indicate the inhomogeneity of the sample, i.e., the existence of both macroscopic regions with different T_c and variations in T_c within such macroscopic regions. The kinks of the steps correspond to the maxima of the derivatives $d\rho/dT$. It can be seen from Table 2 and inset *b*, that with increasing pressure, the $d\rho/dT$ maxima shift to higher temperatures, but the distance between the maxima $((T_c^{high} - T_c^{low}) \approx 0.4)$ does not depend on pressure [48].

Since T_c depends on the oxygen deficiency, δ, and the Pr concentration, it is clear that the pressure within the limits used has very little effect on the distribution of oxygen and praseodymium atoms in the sample.

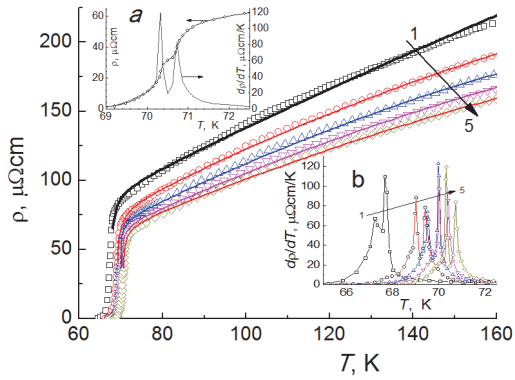

Fig. 4.Temperature dependences of the resistivity in the basal plane of the $Y_{0.77}Pr_{0.23}Ba_2Cu_3O_{7-\delta}$ single crystal at different pressures: *1* — $P = 0$; *2* — 4.1 kbar; *3* — 6.4 kbar; *4* — 8.7 kbar; *5* — 11 kbar. Symbols are the experimental data; lines are the approximations according to (2). Inset a: transition to the superconducting state at P = 11 kbar and the corresponding temperature derivative of the resistivity. Inset b: The temperature derivatives of the resistivity in the SC transition region at various pressures.

Fig. 5 shows the temperature dependences of individual parameters and factors in (2) in the initial state ($P = 0$). It can be seen that in the normal state, the main contribution to the resistivity comes from the intraband scattering ρ_5 and the residual resistance ρ_0. The contributions from the interband scattering ρ_3 and the corrections associated with a change in the shape of the curve of the density of electronic states (1 –

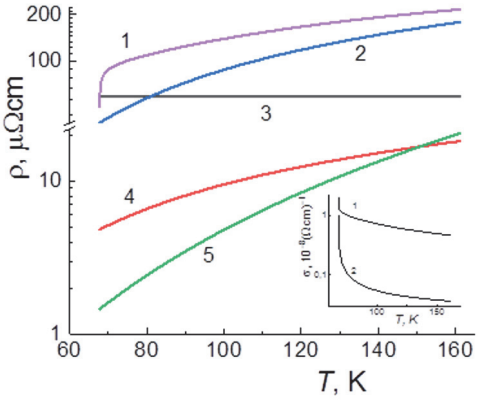

Fig. 5. Temperature dependences of values of parameters in (2) for $P = 0$: *1* — total resistivity $\rho(T)$; *2* — ρ_5; *3* — ρ_0; *4* — ρ_3; *5* — $(1 - b_0T^2)$. Inset: *1* — total conductivity $1/\rho(T)$; *2* — $\Delta\sigma_{LD}$.

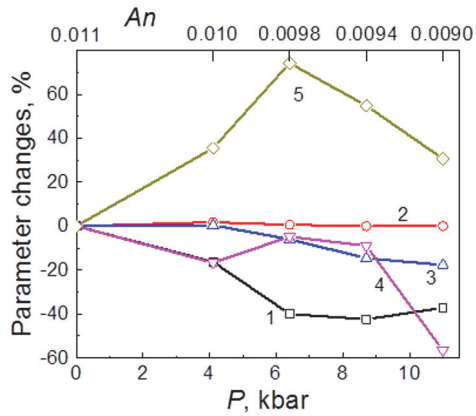

Fig. 6. Relative changes in approximation parameters from (2) depending on pressure P (lower scale) or anisotropy of linear compressibility $An = [c/3 - (a + b)/2]/V^{1/3}$ (upper scale). *1* — ρ_0; *2* — θ; *3* — C_5; *4* — C_3; *5* — b_0.

b_0T^2) are an order of magnitude smaller. The inset in Fig. 5 shows the temperature behavior of the conductivity in the Lorentz-Doniach model [46], $\Delta\sigma_{LD}$, in comparison with the total conductivity of the sample in the normal state, $\rho_{ab}(T, P = 0)$. It is seen that at temperatures below a certain one (in this case, at $T \leq 68$ K), the value $\Delta\sigma_{LD}$ prevails.

According to [47, 49], at the pressure values we used, the relative decrease in the sample volume does not exceed 1 %, while a relative decrease in the approximation parameters (2) is much larger (Table 2). This means that the effect of pressure on the resistivity of the sample is due not so much to a change in the density of the conduction electrons as to a change in the electronic structure.

In the previous work [47] it was noted that $YBa_2Cu_3O_{7-\delta}$ compounds are characterized by a significant anisotropy of linear compressibility in the directions along and perpendicular to the c axis. This anisotropy of compressibility decreases with increasing pressure and characterized by the equation $An = [c/3 - (a + b)/2]/V^{1/3}$ (a, b and c are the unit cell parameters) [47]. Fig. 6 shows the relative changes in the approximation parameters from (2) at different pressures P, (lower scale) and anisotropy of linear compressibility, An, (upper scale).

In [50], a geometric crossover indicates a transition from the 3D regime at $\xi(T) << h$ (h is the film thickness) to the 2D regime at $\xi(T) > h$ with decreasing temperature. In [51], a decrease in the anisotropy in $Sr_{14-x}Ca_xCu_{24}O_{41+\delta}$ with increasing pressure was associated with the transition from one-dimensional to two-dimensional conductivity. The decrease in the anisotropy in $Y_{0.77}Pr_{0.23}Ba_2Cu_3O_{7-\delta}$ with increasing pressure is due to a rapid decrease in the interplanar spacing c in comparison with a and b parameters. At high pressures, this process can lead to a "baric" crossover from 3D to 2D regime by reducing the interplanar spacing to $c \leq \xi(T)$, when pressure is applied.

Fig. 6 shows that under pressure, the greatest relative change is observed for the parameter b_0, which, according to [45], depends on the shape of the curve of the density of electron states on the Fermi surface; parameters ρ_0, C_5 and C_3 show a tendency to decrease with increasing pressure or with decreasing anisotropy; the Debye temperature, θ, obtained from the Bloch-Gruneisen relation does not depend on pressure.

Since $\Delta\theta/\theta \approx \Delta V/V + \Delta F/F$ ($\Delta F/F$ is the magnitude of the interatomic interaction), the constancy of θ (at $\Delta V/V < 0$) means that in the range of used pressures (and for the corresponding change in the anisotropy of the linear compressibility) $\Delta F/F \approx |\Delta V/V$, i.e. the increase in the interatomic interaction compensates for the decrease in volume.

It was shown [52] that to describe the phonon heat capacity of $RBa_2Cu_3O_x$ samples, three Debye temperatures should be introduced: θ_1 corresponding to transverse fluctuations propagating along the c axis; θ_2 corresponding to transverse fluctuations propagating perpendicular to the c axis; and θ_3 corresponding to longitudinal fluctuations at that $\theta_3 \sim \theta_2 > \theta_1$. For $YBa_2Cu_3O_x$: $\theta_1 = 90$ K, $\theta_2 = 850$ K, and $\theta_3 = 295$ K.

As can be seen from Table 2, for our sample, $\theta \approx 280$ K, i.e. charge carriers are scattered mainly by longitudinal fluctuations. Since longitudinal fluctuations are always associated with deformations in all three directions, a decrease in anisotropy with increasing pressure affected them rather weakly, which caused the Debye temperature θ to be constant.

The values of T_c and θ obtained from the experimental dependences $\rho(T)$ make it possible to determine the electron-phonon interaction constant λ from the McMillan relation [53, 54]:

$$T_c = \frac{\theta}{1.45}\exp[-\frac{1.04(1+\lambda)}{\lambda - \mu^*(1 + 0.62\lambda)}], \quad (3)$$

where μ^* is the effective Coulomb repulsion. However, from (3) it follows that there is a maximum value of the T_c/θ ratio: $(T_c/\theta)_{max} \approx 0.2438$ at $\mu^* = 0$ and $\lambda \to \infty$. According to our data, the T_c^{high}/θ ratio increases from 0.242 to 0.254, that is, either it corresponds to unrealistically large values of λ or does not correspond to equation (3) at all. In our opinion, the real phonon spectrum of an anisotropic $Y_{0.77}Pr_{0.23}Ba_2Cu_3O_{7-\delta}$ single crystal cannot be described by the Debye model, and the parameter θ obtained from fitting relations (3) to the experimental values $\rho_{ab}(T)$ characterizes the type of fluctuations on which charge carriers are scattered. Note that in [55], where the Debye temperature in polycrystalline YBa2Cu3Ox was determined from the spin-lattice relaxation time, the value of θ varied from 450 K to 280 K for T_c from 74.7 K to 56.3 K, which corresponds to T_c/θ from 0.166 to 0.201. From McMillan's formula, it was found that λ varies from 4 to 10, respectively. It is clear that the adequacy of the McMillan formula is determined in this case by the value of θ which turned out to be greater in an isotropic polycrystal than in an anisotropic single crystal.

Table 2 also shows that the interplanar pairing constant, $J = (2\xi_c(0)/d)^2$, does not depend on pressure. Taking into account the dependence $c(P)$ [47], the calculated average value of the coherence length is $\xi_c(0) = (21\pm3)$ 9∞. This is an order of magnitude higher than the value obtained in [48]. This discrepancy is probably due to the method of separating excess conductivity. In [48], the excess conductivity was determined by subtracting the high-temperature conductivity, extrapolated to a low temperature, from the experimental values; and here the excess conductivity was determined by subtracting the conductivity calculated by the formula (2) from the experimental values of ρ^{-1}. The large error in the value $\langle J \rangle$ is most likely associated with the inhomogeneity of the sample (see inset *a* in Fig. 4).

We note that the application of pressure also leads to a considerable (up to 17 K) broadening of the linear section in the $\rho_{ab}(T)$ plot at higher temperatures. The latter is expressed in a decrease of the temperature T^* at which experimental points begin to systematically deviate downward from the linear dependence. According to the modern concepts, T^* corresponds to the pseudogap opening temperature [1, 8], as will be described in detail below.

A faster than linear decrease in $\rho_{ab}(T)$ observed at $T < T^*$ reflects the appearance of the so-called excess conductivity $\Delta\sigma$ in the crystal. The temperature dependence of the excess conductivity is determined [1, 8] from the relation:

$$\Delta\sigma = \sigma - \sigma_{lin}, \quad (4)$$

where $\sigma_{lin} = \rho_{lin}^{-1} = (A + BT)^{-1}$ is the conductivity determined via extrapolation of the linear section of$\rho_{ab}(T)$ toward zero temperature, and $\sigma = \rho^{-1}$ is the experimentally measured value of the conductivity in the normal state.

In the rather wide temperature range, these dependences have a linear section that allows for their description with an exponential dependence:

$$\Delta\sigma \sim \exp(\Delta^*_{ab}/T), \quad (5)$$

where Δ^*_{ab} determines some thermally activated process over the energetic gap — pseudogap.

At present, the most widely discussed mechanisms for the pseudogap state in HTS cuprates are represented by the concept of uncorrelated pairs [1, 56] and various models of dielectric fluctuations [57]. Here, one should especially mention the theory of crossover from the BCS mechanism to the mechanism of Bose-Einstein condensation (BEC) [56]. Within the framework of this theory, temperature dependences of the pseudogap were obtained for the cases of strong and weak coupling. In the general

form, these dependences are described by the equation:

$$\Delta(T) = \Delta(0) - \Delta(0)\sqrt{\frac{\pi}{2}}\sqrt{\frac{T}{\Delta(0)}}\exp[-\{\Delta\frac{(0)}{T}] \times \left[1 + erf\left(\sqrt{\frac{\sqrt{x_0^2+1} - 1}{T/\Delta(0)}}\right)\right], \quad (6)$$

where $x_0 = \mu/\Delta(0)$ (μ is the chemical potential; $\Delta(0)$ is the energy gap at $T = 0$), and $erf(x)$ is the error function.

In the limiting case of weak pairing [56], Eq. (6) is reduced to:

$$\Delta(T) = \Delta(0) - \Delta(0)\sqrt{2\pi\Delta(0)T}\exp\left[-\frac{\Delta(0)}{T}\right], \quad (7)$$

which is well known in the BCS theory.

In the BEC limit of strong pairing [56], in the 3D case, $x_0 < -1$, Eq. (6) acquires the form:

$$\Delta(T) = \Delta(0) - \frac{8}{\sqrt{\pi}}\sqrt{-x_0}\left(\frac{\Delta(0)}{T}\right)^{3/2}\exp\left[-\frac{\sqrt{\mu^2 + \Delta^2(0)}}{T}\right]. \quad (8)$$

Herewith, as it was shown in [1, 8, 17, 20, 58], if the measurements are done accurately enough, the pseudogap values in a wide temperature range can be deduced from the $\rho_{ab}(T)$ data at $T < T^*$. The exponential dependence $\Delta\sigma(T)$ was previously observed for YBCO films [58]. As it was shown in [58], fitting of the experimental data can be substantially improved by introducing a prefactor $(1 - T/T^*)$. In this case, the excess conductivity appears proportional to the density of superconducting carriers $n_s \sim (1 - T/T^*)$ and inversely proportional to the number of pairs $\sim \exp(-\Delta^*/kT)$ broken by thermal motion:

$$\Delta\sigma \sim (1 - T/T^*)\exp(\Delta^*_{ab}/T). \quad (9)$$

Here, T^* is considered as the mean-field superconducting transition temperature. The temperature interval $T_c < T^*$ of the pseudogap state is determined by the phase rigidity of the order parameter, which in turn depends on the oxygen deficiency and the dopant concentration. In this way, adopting the approach suggested in [58] the experimental curve $\ln\Delta\sigma$ allows one to deduce the temperature dependence $\Delta^*_{ab}(T)$ up to T^*.

Fig. 7 shows the temperature dependences of the pseudogap for a number of pressures as $\Delta^*(T)/\Delta_{max}$ versus T/T^*. Here, Δ_{max} is the value of Δ^* on the plateau far away from T^*. The dependences $\Delta^*(T)/\Delta(0)$ on T/T^* calculated by Eqs. (7) and (8) in the mean-field approximation within the framework of the BCS crossover theory [56] for the crossover parameter $\mu/\Delta(0) = 10$ (BSC limit), -2, -5, -10 (BEC limit) are shown by dashed lines in Fig. 7. With an increase in pressure, experimental curves develop from dependences described by Eq. (8) to those described by Eq. (7). This behavior turns out to be qualitatively similar to the transformation of the temperature dependences of the pseudogap of YBCO single crystals upon a decrease in the degree of oxygen non-stoichiometry [4, 35]. These correlations $\Delta^*(T)$ do not seem to be accidental. Indeed, as is known from the literature (see, e.g. [1, 2, 19, 20]), to type 1-2-3 HTSC, as well as an increase of the oxygen content [17, 22], leads to enhancements of the conducting characteristics, which manifests itself in an increase of T_c and a decrease in ρ. In this way, with some conventionality in determining T^* from the deviation of $\rho_{ab}(T)$ from the linear dependence, the agreement between experiment and theory in our case can be considered satisfactory.

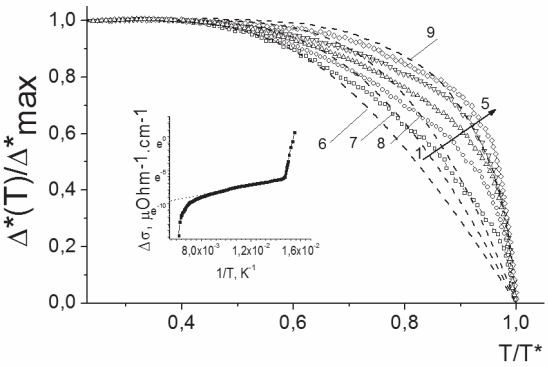

Fig. 7. Temperature dependences of the pseudogap in the reduced coordinates $\Delta^*(T)/\Delta^*_{max}$ versus T/T^* for the $Y_{0.77}Pr_{0.23}Ba_2Cu_3O_{7-\delta}$ single crystal (Δ^*_{max} is the Δ^* far away from T^* on the plateau). The numbering of the curves corresponds to Fig. 4. The dependences $\Delta^*(T)/\Delta(0)$ on T/T^* calculated according to [56] for the crossover parameter $\mu/\Delta(0) = 10$ (BCS limit), -2, -5, -10 (BEC limit) are shown by dashed lines 6–9, respectively.

As we can see from insert to Fig. 7, excess conductivity has a strong increase near T_c. The excess conductivity near T_c is probably due to the processes of fluctuation pairing of the charge carriers and can be described in terms of the Lawrence-Doniach

model [46]. This model assumes the presence of a very smooth crossover from the 2D to the 3D regime of fluctuation conductivity with decreasing temperature of the sample:

$$\Delta\sigma = \left[\frac{e^2}{16hd}\right]\varepsilon^{-1}\left\{1 + J\varepsilon^{-1}\right\}^{-1/2}, \qquad (10)$$

where $\varepsilon = (T - T^{mf}{}_c)/T^{mf}{}_c$ is the reduced temperature; $T^{mf}{}_c$ is the critical temperature in the mean-field approximation; $J = (2\xi_c(0)/d)^2$ is the interlayer coupling constant; ξ_c is the coherence length along the c-axis, and d is the thickness of the 2D layer. Near T_c, when $\xi_c \le d$, the interaction between fluctuational Cooper pairs is realized in the entire sample volume, that corresponds to the 3D regime. The 2D regime is realized when $\xi_c > d$ and the interaction is only possible within the planes of the conducting layers. Accordingly, in the limiting cases, Eq. (10) is transformed into the known relations for the 3D and 2D cases, obtained in terms of the Aslamazov-Larkin theory [50]:

$$\Delta\sigma_{2D} = \frac{e^2}{16hd}\varepsilon^{-1}, \qquad (11)$$

$$\Delta\sigma_{3D} = \frac{e^2}{32h\xi_c(0)}\varepsilon^{-1/2}. \qquad (12)$$

An accurate determination of $T^{mf}{}_c$, which strongly affects the slope of $\Delta\sigma(\varepsilon)$, is essential for comparison of experiment with theory. In such a procedure, $\xi_c(0)$, d and T_c in Eqs. (10)–(12) are usually varied as fitting parameters [59]. However, this approach often results in quantitative discrepancies between theory and experiment. This requires the inclusion of some scaling term as an additional fitting parameter. This so-called C-factor makes it possible to improve the agreement with the experimental data and, thus, take into account the possible inhomogeneity in the distribution of the transport current in the system under consideration. In our analysis, for $T^{mf}{}_c$ we used the values of T_c at the points of maxima in $d\rho_{ab}/dT$ in the region of the superconducting transition [2].

The temperature dependences $\Delta\sigma(T)$ are presented in Fig. 8 as $\ln\Delta\sigma$ versus $\ln\varepsilon$. Near T_c, these dependences are satisfactory approximated by straight lines with a slope

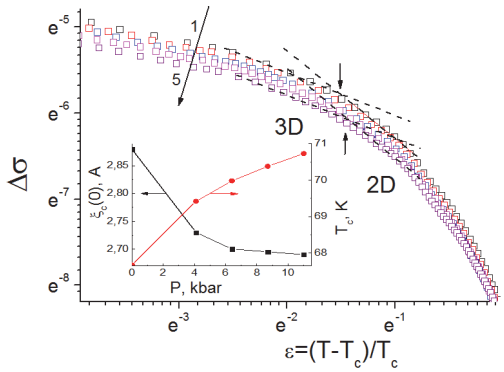

Fig. 8. Temperature dependences $\Delta\sigma(T)$ for *a* series of pressures in the $\ln\Delta\sigma$ versus $\ln\varepsilon$ representation. Curve numbering corresponds to Fig. 4. Inset: Dependences $T_c(P)$ and $\xi_c(P)$.

$\alpha_1 \approx -0.5$, corresponding to the exponent 1/2 in Eq. (12), which indicates the 3D character of the fluctuation conductivity in this temperature range. With a further increase in temperature, $\Delta\sigma$ decreases faster ($\alpha_2 \approx -1$), which indicates the dimensionality change in the fluctuation conductivity. From (11) and (12), it follows that at the 2D–3D crossover point:

$$\varepsilon_0 = 4\left[\xi_c(0)/d\right]^2. \qquad (12)$$

Thus, from the determined value of ε_0 and literature data for the dependence of T_c and the interlayer distance on δ [60, 61] one can calculate the value of $\xi_c(0)$.

As follows from the inset to Fig. 4, $\xi_c(0)$ calculated by Eq. (12) decreases from 2.88 Å to 2.69 Å with increasing T_c. This qualitatively differs from the pressure dependences of $\xi_c(0)$ obtained for impurity-free YBCO samples of an optimal composition [17, 22] and for single crystals lightly doped with Pr [8, 20]. Namely, for optimally-doped YBCO single crystals, $\xi_c(0)$ only slightly varies with an increase in pressure [2, 22]. At the same time, for single crystals lightly doped with Pr [20], $\xi_c(0)$ exhibits an increase by about 15 % with increasing pressure from 0 to 17 kbar. It should also be noted that in our work, there is a clear correlation in the behavior of the dependences $\xi_c(P)$ and $T_c(P)$ with an increase in pressure (see the inset to Fig. 8). Both these physical values change simultaneously; namely, an increase in $T_c(P)$ is accompanied by a decrease in $\xi_c(P)$, that may

indicate the same nature of the change in these characteristics.

Conclusions

As a result of the studies performed, it can be concluded that doping with praseodymium leads to an anisotropic distribution of defects: flat macroscopic superconducting regions with different T_c are formed. Macroscopic inhomogeneities cause the formation of a multistep superconducting transition, shifted to the region of lower temperatures; the steps of this transition are longer than during the initial transition due to the enhancement of mesoscopic inhomogeneities. An increase in the concentration of praseodymium leads to a decrease in the localization length of charge carriers, which indicates a decrease in the spatial propagation of the wave function of charge carriers. In the normal state, the main contribution to the resistivity of the $Y_{0.77}Pr_{0.23}Ba_2Cu_3O_{7-\delta}$ single crystal is due to intraband scattering ($\propto T^5$) and residual resistivity. Hydrostatic pressure leads to a decrease in the anisotropy of linear compressibility together with a decrease in residual resistivity and phonon resistivity; the Debye temperature and coherence length remain constant. The superconducting transition and Debye temperatures obtained from the experimental temperature dependence of the resistivity do not correspond to the McMillan formula, probably due to the large anisotropy. In general, the application of high pressure to $Y_{1-x}Pr_xBa_2Cu_3O_{7-\delta}$ single crystals with moderate Pr doping levels ($x \approx 0.23$) leads to an essential broadening of the linear section of the dependence $\rho_{ab}(T)$, corresponding to narrowing of the pseudogap temperature range. Herewith, the excess conductivity obeys an exponential temperature dependence in a broad range of temperatures, while the temperature dependence of the pseudogap is satisfactory described within the BCS-BEC crossover theory. The pressure-induced evolution of the fluctuation conductivity in lightly Pr-doped $Y_{1-x}Pr_xBa_2Cu_3O_{7-\delta}$ single crystals seems to be determined by two processes: the general "three-dimensionality" of the system, due to the evolution of the relationship between ξ_c and d and due to the doping of Pr with a shift of the Fermi level relative to the features of the density of states. Thus, in contradistinction with impurity-free and lightly Pr-doped YBCO samples, the application of high pressure leads to a substantial increase in the pressure derivatives dT_c/dP and $d\xi_c/dP$.

References

1. R.V.Vovk, A.L.Solovyov, *Low Temperature Physics*, **44**, 81 (2018). https://doi.org/10.1063/1.5020905.
2. L.Mendonca Ferreira, P.Pureur, H.A.Borges, P.Lejay, *Phys. Rev. B*, **69**, 212505 (2004).
3. J.G.Bednorz, K.A.Muller, *Zeitschrift fur Physik B — Condensed Matter*, **64**, 189 (1986).
4. Yu.I.Boyko, V.V.Bogdanov, R.V.Vovk, B.V.Grinyov, *Funct. Mater.*, **27**, 703 (2020).
5. Yu.I.Boyko, V.V.Bogdanov, R.V.Vovk, B.V.Grinyov, *Funct. Mater.*, **28**, 415 (2021).
6. J.Ashkenazi, *J. Supercond. Nov. Magn.*, **24**, 1281 (2011).
7. M.Akhavan, *Physica B*, **321**, 265 (2002).
8. R.V.Vovk, M.A.Obolenskiy, A.A.Zavgorodniy et al., *Physica B*, **404**, 3516 (2009).
9. M.K.Wu, J.R.Ashburn, C.J.Torng et al., *Phys. Rev. Lett.*, **58**, 908 (1987).
10. A.V.Bondarenko, V.A.Shklovskij, R.V.Vovk et al., *Low Temperature Physics*, **23**, 962 (1997).
11. R.V.Vovk, G.Ya.Khadzhai, O.V.Dobrovolskiy, *Appl. Phys. A*, **117**, 997 (2014). DOI:10.1007/s00339-014-8670-2.
12. R.V.Vovk, Z.F.Nazyrov, L.I.Goulatis, A.Chroneos, *Journal of Low Temperature Physics*, **170**, 216 (2013). DOI:10.1007/s10909-012-0755-8
13. G.Ya.Khadzhai, N.R.Vovk, R.V.Vovk, *Low Temperature Physics*, **40**, 488 (2014). https://doi.org/10.1063/1.4881197
14. R.V.Vovk, N.R.Vovk, G.Ya.Khadzhai et al., *Solid State Communications*, **190**, 18 (2014). http://dx.doi.org/10.1016/j.ssc.2014.04.004.
15. R.V.Vovk, N.R.Vovk, G.Ya.Khadzhai et al., *Current Applied Physics*, **14**, 1779 (2014).
16. R.V. Vovk, N.R.Vovk, A.V.Samoilov et al., *Solid State Communications*, **170**, 6 (2013). http://dx.doi.org/10.1016/j.ssc.2013.07.011.
17. A.L.Solovjov, E.V.Petrenko, L.V.Omelchenko et al., *Scientific Reports*, **9**, 9274 (2019).
18. D.A.Lotnyk, R.V.Vovk, M.A.Obolenskii et al., *Journal of Low Temperature Physics*, **161**, 387 (2010). DOI 10.1007/s10909-010-0198-z.
19. D.D.Balla, A.V.Bondarenko, R.V.Vovk et al., *Low Temp.Phys.*, **23**, 777 (1997).
20. A.L.Solovjov, L.V.Omelchenko, E.V.Petrenko et al., *Scientific Reports*, **9**, 20424 (2019). https://doi.org/10.1038/s41598-019-55959-1.
21. R.P.Gupta, M.Gupta, *Phys. Rev. B*, **51**, 11760 (1995).
22. R.V.Vovk, N.R.Vovk, G.Ya.Khadzhai et al., *Physica B*, **422**, 33 (2013). http://dx.doi.org/10.1016/j.physb.2013.04.032.
23. S.Sadewasser, J.S.Schilling, A.P.Paulicas, B.M.Veal, *Phys. Rev. B*, **61**, 741 (2000).
24. R.V.Vovk, G.Ya.Khadzhai, Z.F.Nazyrov et al., *Physica B*, **407**, 4470 (2012).

25. W.-H.Li, S.Y.Wu, Y.-C.Lin et al., *Phys. Rev. B*, **60**, 4212 (1999).
26. R.V.Vovk, N.R.Vovk, G.Ya.Khadzhai, O.V.Dobrovolskiy, *Solid State Communication*, **204**, 64 (2015).
27. G.Ya.Khadzhai, A.Chroneos, I.L.Goulatis et al., *Journal of Low Temperature Physics*, **203**, 430 (2021). https:doi.org/10.1007/s10909-021-02590-y.
28. J.M.Ziman, Electrons and Phonons, Oxford at the Clarendon Press (1960).
29. I.V.Alexandrov, A.F.Goncharov, S.M.Stishov, *JETP Letters*, **47**, 428 (1988).
30. M.A.Ivanov, V.M.Loktev, *Low Temperature Physics*, **25**, 996 (1999). https://doi.org/10.1063/1.593854
31. G.Ya.Khadzhai, C.R.Vovk, R.V.Vovk, *Low Temperature Physics*, **43**, 1119 (2017). https://doi.org/10.1063/1.5004458
32. S.Kirkpatrick, *Rev. Mod. Phys.*, **45**, 574 (1973).
33. J.Maza, F.Vidal, *Phys. Rev. B*, **43**, 10560 (1991). https://doi.org/10.1103/PhysRevB.43.10560
34. H.A.Borges, M.A.Continentino, *Solid State Commun.*, **80**, 197 (1991).
35. G.Lacayc, R.Hermann, G.Kaestener, *Physica C*, **192**, 207 (1992).
36. B.N.Rolov, V.E.Jurkiewicz, Physics Blurred Phase Transitions, House Rostov University (1983) [in Russian].
37. W.Kanzig, Ferroelectrics and Antiferroelectrics, Academic Press, New York (1957).
38. A.F.Prekul, V.A.Rassokhin, S.V.Yartsev, *JETP Letters*, **38**, 408 (1983).
39. R.V.Vovk, C.D.H.Williams, A.F.G.Wyatt, *Phys. Rev. B*, **69**, 144524 (2004).
40. A.J.Matthews, K.V.Kavokin, A.Usher et al., *Phys. Rev. B*, **70**, 075317 (2004).
41. D.H.S.Smith, R.V.Vovk, C.D.H.Williams, A.F.G.Wyatt, *Phys. Rev. B*, **72**, 054506 (1-7) (2005).
42. P.G.Curran, V.V.Khotkevych, S.J.Bending et al., *Phys. Rev. B*, **84**, 104507 (2011).
43. N.Kuganathan, P.Iyngaran, R.Vovk, A.Chroneos, *Scientific Reports*, **9**, 4394 (2019). https:doi.org/10.1038/s41598-019-40878-y.
44. L.Colquit, *J.Appl. Phys*, **36**, 2454 (1965). https://doi.org/10.1063/1.17145 10
45. T.Aisaka, M.Shimizu, *J. Phys. Soc. Japan*, **28**, 646 (1970). https://doi.org/10.1143/JPSJ.28.646
46. W.E.Lawrence, S.Doniach, Proc. of the Twelth Intern. Conference on Low Temperature Physics, ed. by E.Kanda, Academic Press of Japan, Kyoto (1971), p.361.
47. Jaja N.Victor, S.Natarajan, G.V.Subba Rao, *Sol. St. Commun.*, **67**, 51 (1988).
48. G.Ya.Khadzhai, N.R.Vovk, R.V.Vovk, *Fiz. Nizk. Temp.*, **47**, 388 (2021). https://doi.org/10.1063/10.0004231
49. V.P.Glazkov, I.N.Goncharenko, V.A.Somenkov, *Solid State Physics*, **30**, 3703 (1988).
50. A.Larkin, A.Varlamov, Theory of Fluctuations in Superconductors, OUP Oxford (2005).
51. H.Takahashi, N.Mori, T.Nakanishi et al., *Rev. High Pressure Sci. Technol.*, **7**, 388 (1998). https://doi.org/10.4131/jshpreview.7.388
52. N.V.Anshukova, Yu.V.Bugoslavskii, V.G.Veselago et al., *JETP Letters*, **48**, 152 (1988).
53. R.C.Dynes, *Solid State Communications*, **10**, 615 (1972). https://doi.org/10.1016/0038-1098(72)90603-5
54. P.B.Allen, R.C.Dynes, *Phys. Rev.B*, **12**, 905 (1975).
55. L.K.Aminov, V.A.Ivanshin, I.N.Kurkin et al., *Physica C*, **349**, 30 (2001).
56. E.Babaev, H.Kleinert, *Phys. Rev. B*, **59**, 12083 (1999).
57. T.Timusk, B.Statt, *Rep. Progr. Phys.*, **62**, 61 (1999).
58. D.D.Prokofiev, M.D.Volkov. Yu.A. Boykov, *Fiz.Tv.Tela*, 45, 1168, (2003)
59. Giapintzakis, D.M.Ginsberg, *Phys. Rev. B*, **39**, 4258 (1989).
60. G.D.Chryssikos, E.I.Kamitsos, J.A.Kapoutsis et al., *Physica C*, **254**, 44 (1995).
61. R.V.Vovk, M.A.Obolenskii, Z.F.Nazyrov et al., *J. Mater Sci.:Mater. Electron.*, **23**, 1255 (2012).